Electrical Power and Energy Systems 64 (2015) 493–504

Contents lists available at ScienceDirect

Electrical Power and Energy Systems

journal homepage: www.elsevier.com/locate/ijepes

An improved control algorithm of DSTATCOM for power quality improvement

Bhim Singh [1], Sunil Kumar Dube *, Sabha Raj Arya [2]

Department of Electrical Engineering, Indian Institute of Technology Delhi, New Delhi 110016, India

ARTICLE INFO

Article history:
Received 6 October 2013
Received in revised form 28 June 2014
Accepted 14 July 2014

Keywords:
Distorted PCC voltages
Adaptive fuzzy logic
Power quality
VSC
Self tuning filter
IRPT

ABSTRACT

This paper presents the modeling and implementation of a three-phase DSTATCOM (Distribution Static Compensator) using STF (Self Tuning Filter) based IRPT (Instantaneous Reactive Power Theory) control algorithm for power quality improvement. It is used for harmonics elimination, load balancing and reactive power compensation at distorted PCC (Point of Common Coupling) voltages under nonlinear loads. An adaptive fuzzy logic controller is used to control the dc bus voltage of VSC (Voltage Source Converter) based DSTATCOM to improve the response and to reduce the overshoot and undershoot of traditional PI (Proportional-Integral) controller under unbalanced loading conditions and supply voltage fluctuations. The effectiveness of the proposed control algorithm is demonstrated through simulation using MATLAB SIMULINK and real time implementation of DSTATCOM conducted using a DSP (Digital Signal Processor dSPACE 1104).

Introduction

Mitigation of power quality problems is the major challenge in present day distribution system [1]. Static power converters such as rectifiers, large number of low-power electronic-based appliances, induction heating, switch mode power supplies, adjustable speed drives, electric traction etc. are nonlinear loads that generate considerable distortions in the AC mains currents and voltages causing power quality problems [2,3]. Chen and Chen [4] have described various control algorithms such as Prony, neural network, PLL (Phase Locked Loop) and others for estimation of various harmonic components on time-varying signals. Various custom power devices and filters are used to mitigate these power quality problems for power factor correction, harmonics compensation, load balancing to the level of international standards [5–7]. One of the custom power device known as DSTATCOM (Distribution Static Compensator) is intensively used for mitigation of current related power quality problems in the distribution systems [8]. The performance of DSTATCOM depends on the design of power circuit components, reference currents estimation algorithms and switching scheme. Tang et al. [9] have described high performance LCL based active filter for reduction of power quality problems. For the performance improvement of an active filter, Bhattacharya et al. [10] have proposed new topology of an active filter operating at different switching frequency for improved performance. A number of publications have reported the performance of active filters under balanced, sinusoidal, unbalanced or distorted AC voltage conditions and their control algorithms [11–15]. In all these attempts, authors have described modeling, application of control algorithms under unbalanced and distorted voltages of AC mains. One of the untraditional applications of the active filter is aircraft power system where frequency is 400 Hz with DSP based control [16] and small hydro generation system [17]. Longhui et al. [18] have described the effect of supply voltage fluctuation on the performance of shunt compensator and feed forward control algorithm is explained to reduce this problem. Ribeiro et al. [19] have introduced adaptive control algorithm which is based on adaptive pole-placement interrogation with variable structure control. Several modifications are suggested by various researchers on IRPT (Instantaneous Reactive Power Theory). Depenbrock et al. [20] have explained instantaneous reactive power component of currents calculation in IRPT current components which do not add to the instantaneous power. Under distorted AC voltages, conventional IRPT has poor performance and its modification in non-ideal supply is suggested by Herrera and Salmeron [21]. SRF based control algorithm [22] suffers from tuning problem of PLL (phase locked loop) and it is also not fully effective in the application of DSTATCOM due to the limitation of PLL.

* Corresponding author. Tel.: +91 8971940725.
E-mail addresses: bsinghrajput56@gmail.com (B. Singh), sun.inie.13@gmail.com (S.K. Dube), sabharaj1@gmail.com (S.R. Arya).
[1] Tel.: +91 01126596225.
[2] Tel.: +91 7838919565.

http://dx.doi.org/10.1016/j.ijepes.2014.07.055
0142-0615/

In the reported literature, Abdusalam et al. [23] have also proposed a control algorithm for reference current estimation under distorted voltages in the application of an active filter with direct current control technique and conventional PI (Proportional Integral) controller for DC bus voltage control under sudden load change and no discussions on effect of supply voltage fluctuations on DC bus voltage has been carried out. Singh et al. [24] have compared two types of current control techniques and it has been shown that the active power filter with indirect current control technique has simple structure, easy to implement in hardware and better harmonics tracking effect than direct current control technique. However, it has also proven in the same literature that indirect current control technique is free from switching ripples and hence it gives better performance during load perturbation whereas in case of direct current control method switching ripples increases with the increase in the load current. Generally the DC capacitor voltage of VSC (Voltage Source Converter) of DSTATCOM is regulated using a PI controller in various control algorithms used for load compensation. However, during load changes, there is a considerable variation in DC capacitor voltage of VSC of DSTATCOM which affects the system performance. Therefore, dynamic performance of traditional PI controller is also not suitable due to serious undesirable oscillations (overshoot and undershoot) and chances of dielectric breakdown of capacitor during transients [25–28]. Under the load variations, the additional power to the load is instantaneously supplied from the DSTATCOM. This leads to a sharp decrease in DC bus capacitor voltage of VSC when the load is suddenly increased and an abrupt increase in DC link capacitor voltage of DSTATCOM when there is momentarily reduction in loads. It is imperative for an optimized compensator to regulate DC bus capacitor voltage close to the reference value as far as possible. The DC bus capacitor voltage of DSTATCOM takes few cycles (normally 6–8) to settle under the disturbances in the loads [29]. The fuzzy logic and adaptive fuzzy logic controllers may be used for improving the dynamics of traditional PI controller to have improved regulation on the DC bus voltage of DSTATCOM, eliminating higher overshoot and undershoot [31–35]. Several publications are reported and compared the performances of different reference current generation strategies under balanced, sinusoidal, unbalanced or distorted alternating current (AC) voltages conditions [36–38]. In all of them, authors have demonstrated that under balanced and sinusoidal AC voltages conditions, the strategies such as the so-called p–q theory and synchronous reference frame theory (SRF) provide similar performances. Differences arise when these are used under distorted and unbalanced AC voltages. In addition, it has been proved in the literature [30] that the supply voltage fluctuations have influence on the DC link voltage and the expression signifying the influence of the change in supply voltage in the change in DC link voltage has also been derived for the shunt active filter. A conventional PI controller used for DC link voltage control suffers from high overshoot and undershoot during the supply voltage fluctuations. However, there is no attempt is made on adaptive fuzzy logic controllers to regulate the dc link voltage along with other parts of the algorithm in case of sudden load changes. In this paper, adaptive fuzzy logic controller is used and is compared with conventional PI controller to reduce the DC link voltage variations in case of supply voltage fluctuations along with the sudden load changes.

In this paper, an improved reference supply currents extraction algorithm for an indirect current control is proposed using a STF (Self Tune Filter) in DSTATCOM under distorted AC mains along with an adaptive fuzzy PI controller to regulate its DC bus voltage. As the proposed control algorithm is based on an indirect current control technique where extraction of fundamental components of load currents has major role in the control, it has less switching ripple in supply currents, superior performance during load perturbations and a simple structure compared to direct current control technique. It improves the dynamic performance due to the elimination of low pass filters. The proposed control algorithm of a DSTATCOM is implemented for the compensation of nonlinear loads in a distribution system with an adaptive fuzzy logic control of DC bus voltage of VSC of DSTATCOM. This effectively performs the functions of DSTATCOM such as reactive power compensation, harmonics attenuation and load balancing. It is observed that the distortions in supply currents are reduced within the specified limit of IEEE-519-1992 even under the distortions in AC mains voltages.

System configuration and control algorithm

Fig. 1 shows a schematic diagram of a three phase VSC based DSTATCOM connected to a three phase distorted voltages of AC mains feeding nonlinear loads with a source impedance (Z_s). For the control of DSTATCOM, sensed input variables are PCC (Point of Common Coupling) voltages of (v_a, v_b, v_c), supply currents (i_{sa}, i_{sb}, i_{sb}), load currents (i_{La}, i_{Lb}, i_{Lc}) and DC bus voltage (v_{dc}) of VSC used in DSTATCOM. Effectiveness of the compensator depends upon the accuracy of extracted fundamental active power and reactive power components of load currents. Interfacing inductors (L_f) are connected at AC output of the VSC for reducing ripple in compensating currents. A three phase series connected capacitor (C_f) and a resistor (R_f) as a passive ripple filter is used at PCC parallel to the loads to suppress high frequency switching noise at PCC voltages caused due to switching of VSC. The DSTATCOM compensating currents (i_{Ca}, i_{Cb}, i_{Cc}) are injected to cancel the reactive power components and harmonics of the load currents. For an effective operation of DSTATCOM, it is necessary to maintain constant DC capacitor voltage of VSC of DSTATCOM. It is realized using an adaptive fuzzy logic based PI controller. The designed value of different auxiliary components of DSTATCOM such as interfacing AC inductors, DC bus voltage and value of DC bus capacitor for simulation and its implementation are given in Appendices A and B respectively.

Fig. 2 shows a block diagram of STF (Self Tuned Filter) based IRPT (Instantaneous Reactive Power Theory) control algorithm for estimation of reference supply currents through the extraction of fundamental load active power and reactive powers.

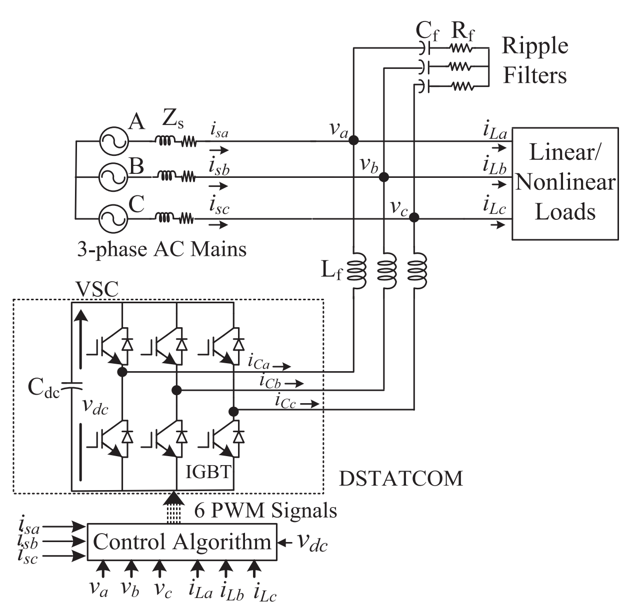

Fig. 1. Schematic diagram of VSC based three phase DSTATCOM.

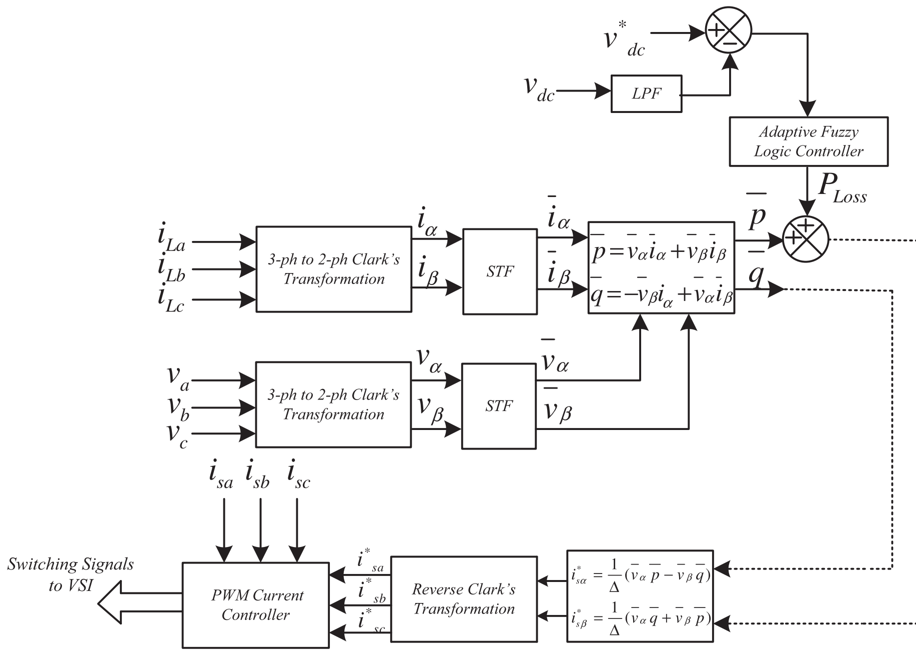

Fig. 2. Reference supply currents estimation using STF based IRPT control algorithm.

Extraction of fundamental PCC voltages and reference supply currents using Self Tuning Filter (STF)

The three-phase distorted PCC voltages can be written in term of fundamental components and distortion as,

$$v_a(t) = V_{a1}\sin(wt + \phi_{a1}) + \sum_{n=2}^{\infty} V_{an}\sin(nwt + \phi_{an}) \tag{1a}$$

$$v_b(t) = V_{b1}\sin\left(wt + \phi_{b1} - \frac{2\pi}{3}\right) + \sum_{n=2}^{\infty} V_{bn}\sin\left(nwt + \phi_{bn} - \frac{2\pi}{3}\right) \tag{1b}$$

$$v_c(t) = V_{c1}\sin\left(wt + \phi_{c1} + \frac{2\pi}{3}\right) + \sum_{n=2}^{\infty} V_{cn}\sin\left(nwt + \phi_{cn} + \frac{2\pi}{3}\right) \tag{1c}$$

where V_{a1}, V_{b1} and V_{c1}, Φ and n are the amplitudes of three phase fundamental PCC voltages, phase delay and order of harmonics respectively.

These PCC voltages of a three-phase system can be transformed into α–β co-ordinates using Clark's transformation as follows,

$$\begin{bmatrix} v_\alpha \\ v_\beta \end{bmatrix} = \sqrt{\frac{2}{3}} \begin{bmatrix} 1 & -1/2 & -1/2 \\ 0 & \sqrt{3}/2 & -\sqrt{3}/2 \end{bmatrix} \begin{bmatrix} v_a \\ v_b \\ v_c \end{bmatrix} \tag{2}$$

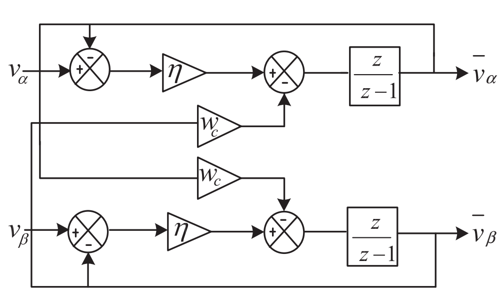

Fig. 3. Self tuned filter tune to fundamental frequency (w_c).

where α–β axes are the orthogonal co-ordinates.

$$\begin{aligned}
v_\alpha(t) &= \sqrt{\frac{2}{3}}v_a(t) - \frac{1}{\sqrt{6}}v_b(t) - \frac{1}{\sqrt{6}}v_c(t) \\
&= \sqrt{\frac{2}{3}}\left\{V_{a1}\sin(wt + \phi_{a1}) + \sum_{n=2}^{\infty}V_{an}\sin(nwt + \phi_{an})\right\} \\
&\quad - \frac{1}{\sqrt{6}}\left\{V_{b1}\sin\left(wt + \phi_{b1} - \frac{2\pi}{3}\right) + \sum_{n=2}^{\infty}V_{bn}\sin\left(nwt + \phi_{bn} - \frac{2\pi}{3}\right)\right\} \\
&\quad - \frac{1}{\sqrt{6}}\left\{V_{c1}\sin\left(wt + \phi_{c1} + \frac{2\pi}{3}\right) + \sum_{n=2}^{\infty}V_{cn}\sin\left(nwt + \phi_{cn} + \frac{2\pi}{3}\right)\right\} \\
&= V_1\left[\sqrt{\frac{2}{3}}\sin(wt + \phi_1) - \frac{1}{\sqrt{6}}\sin\left(wt + \phi_1 - \frac{2\pi}{3}\right)\right. \\
&\quad \left. - \frac{1}{\sqrt{6}}\sin\left(wt + \phi_1 + \frac{2\pi}{3}\right)\right] \\
&\quad + V_n\left[\sqrt{\frac{2}{3}}\sum_{n=2}^{\infty}\sin(nwt + \phi_n) - \frac{1}{\sqrt{6}}\sum_{n=2}^{\infty}\sin\left(nwt + \phi_n - \frac{2\pi}{3}\right)\right. \\
&\quad \left. - \frac{1}{\sqrt{6}}\sum_{n=2}^{\infty}\sin\left(nwt + \phi_n + \frac{2\pi}{3}\right)\right] \\
&= \left(\sqrt{\frac{2}{3}} + \frac{1}{\sqrt{6}}\right)\sin wt\cos\phi_1 + \left(\sqrt{\frac{2}{3}} + \frac{1}{\sqrt{6}}\right)\cos wt\sin\phi_1 \\
&\quad + \left(\sqrt{\frac{2}{3}} + \frac{1}{\sqrt{6}}\right)\sin nwt\cos\phi_n + \left(\sqrt{\frac{2}{3}} + \frac{1}{\sqrt{6}}\right)\cos nwt\sin\phi_n \\
&= \sqrt{\frac{3}{2}}V_1\sin(wt + \phi_1) + \sqrt{\frac{3}{2}}\sum_{n=2}^{\infty}V_n\sin(nwt + \phi_n)
\end{aligned}$$

Similarly $v_\beta(t)$ can also be derived from Eqs. (1) and (2). Therefore, one is having following two equations,

$$v_\alpha(t) = \sqrt{\frac{3}{2}}V_1\sin(wt + \phi_1) + \sqrt{\frac{3}{2}}\sum_{n=2}^{\infty}V_n\sin(nwt + \phi_n) \tag{3}$$

$$v_\beta(t) = -\sqrt{\frac{3}{2}}V_1\cos(wt + \phi_1) - \sqrt{\frac{3}{2}}\sum_{n=2}^{\infty}V_n\cos(nwt + \phi_n) \tag{4}$$

where V_1 and V_n are the magnitude of fundamental component of PCC voltages, Φ and n are phase delay and order of harmonics respectively.

It can also be expressed as,

$$v_{\alpha\beta s}(t) = v_{\alpha\beta e}(t)e^{jwt} \tag{5}$$

where $v_{\alpha\beta s}(t)$ and $v_{\alpha\beta e}(t)$ are the instantaneous voltage signals in stationary reference frame and SRF (Synchronously Rotating Reference Frame) of wt respectively [39–42].

The above equation can be expressed by the following transfer function,

$$H(t) = \frac{v_{\alpha\beta s}(t)}{v_{\alpha\beta e}(t)} = e^{jwt} \tag{6}$$

Applying Laplace's Transformation in the above transfer function, one can get the following relation as,

$$H(s) = \frac{v_{\alpha\beta s}(s)}{v_{\alpha\beta e}(s)} = \frac{s + jw}{s^2 + w^2} \tag{7}$$

In the above transfer function to get the stationary component one needs to track the rotating phase angle vector (wt) which needs PLL (Phase Lock Loop) creating phase delay.

Therefore to eliminate the above problem by the addition of a constant η in the above transfer function one can obtain a STF with a cut-off frequency w_c which can be written as,

$$H(s) = \frac{v_{\alpha\beta s}(s)}{v_{\alpha\beta e}(s)} = \eta\frac{(s+\eta) + jw_c}{(s+\eta)^2 + w_c^2} \tag{8}$$

Simplifying the above transfer function and applying Inverse Laplace's Transform it can be written as,

$$v_{\alpha\beta s}(t) = \eta e^{-\eta t}e^{jw_c t} * v_{\alpha\beta e}(t) \tag{9}$$

Replacing $v_{\alpha\beta s}(t)$ by $\bar{v}_\alpha(t) + j\bar{v}_\beta(t)$ and the output signals $v_{\alpha\beta e}(t)$ by $v_\alpha(t) + jv_\beta(t)$, the following equations can be obtained as,

$$\bar{v}_\alpha(t) + j\bar{v}_\beta(t) = \{\eta e^{-\eta t}\cos(w_c t) + j\eta e^{-\eta t}\sin(w_c t)\} \times \{v_\alpha(t) + jv_\beta(t)\} \tag{10}$$

Equating real and imaginary parts one can write as follows,

$$\bar{v}_\alpha(t) = \eta e^{-\eta t}\{v_\alpha(t)\cos(w_c t) - v_\beta(t)\sin(w_c t)\} \tag{11}$$

$$\bar{v}_\beta(t) = \eta e^{-\eta t}\{v_\alpha(t)\sin(w_c t) + v_\beta(t)\cos(w_c t)\} \tag{12}$$

These two equations for the mth sampling period can be expressed as,

$$\bar{v}_\alpha(mT_s) = \eta e^{-\eta mT_s}\{v_\alpha(mT_s)\cos(w_c mT_s) - v_\beta(mT_s)\sin(w_c mT_s)\} \tag{13}$$

$$\bar{v}_\beta(mT_s) = \eta e^{-\eta mT_s}\{v_\alpha(mT_s)\sin(w_c mT_s) + v_\beta(mT_s)\cos(w_c mT_s)\} \tag{14}$$

where 'T_s' is the sampling period and 'm' is the sampling number.

The detailed expressions of Eqs. (11) and (12) as an output of STF i.e. $\bar{v}_\alpha(t)$ and $\bar{v}_\beta(t)$ are given in Appendix C.

Simplifying Eqs. (11) and (12) and using Laplace transformation one can expressed as follows,

$$\bar{v}_\alpha(s) = \frac{\eta}{s}\{v_\alpha(s) - \bar{v}_\alpha(s)\} - \frac{w_c}{s}\bar{v}_\beta(s) \tag{15}$$

$$\bar{v}_\beta(s) = \frac{\eta}{s}\{v_\beta(s) - \bar{v}_\beta(s)\} + \frac{w_c}{s}\bar{v}_\alpha(s) \tag{16}$$

These Eqs. (15) and (16) are used to extract the fundamental component from distorted voltages signals without any phase delay and amplitude change. The block diagram representation of STF tuning to fundamental frequency (w_c) in discrete time domain is shown in Fig. 3.

In Fig. 4, the Bode plot of STF for different values of parameter η is demonstrated. One can notice that small value of 'η' increases filter selectivity. Moreover, one can observe that no displacement is introduced by this filter at the system fundamental frequency of f_c = 50 Hz. Therefore, one can observe that STF eliminates the frequency components higher than the fundamental frequency (f_c = 50 Hz) and the fundamental component can be extracted from distorted electrical signals (voltage or current) without any phase delay and change of amplitude. Hence taking this and Appendix C into considerations, the value of 'η' is taken as 20 for optimum performance of STF.

The currents in the α–β axis can be decomposed into fundamental AC and oscillatory components as,

$$\begin{aligned} i_\alpha(t) &= \bar{i}_\alpha(t) + \tilde{i}_\alpha(t) \\ i_\beta(t) &= \bar{i}_\beta(t) + \tilde{i}_\beta(t) \end{aligned} \tag{17}$$

The STF extracts the fundamental components at the frequency w_c directly from the load currents in a similar manner in case of PCC voltages in the α–β axis which are composed of fundamental AC as well as oscillatory components.

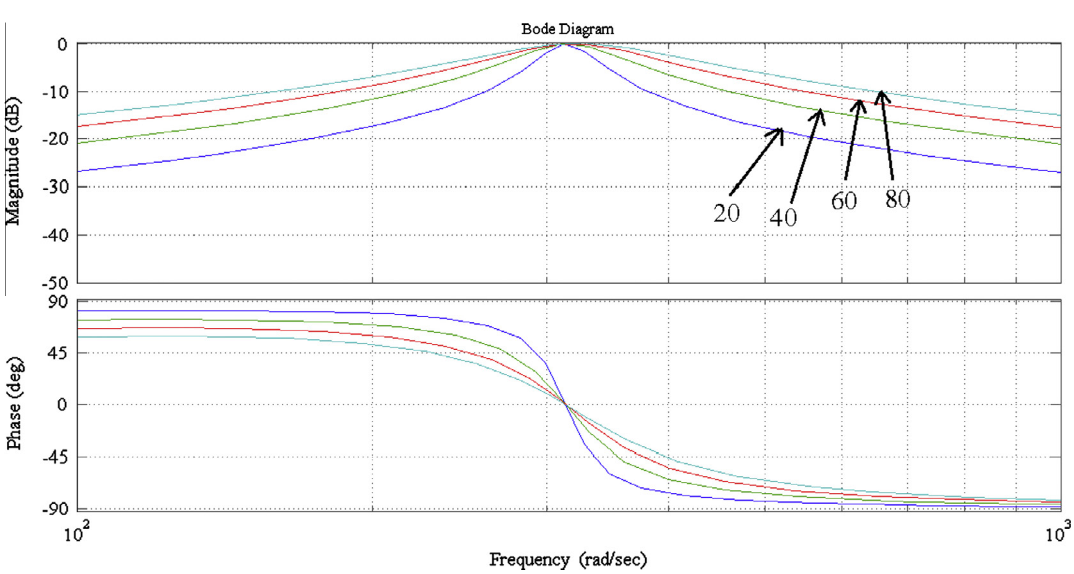

Fig. 4. Bode plot of STF for different values of parameter η.

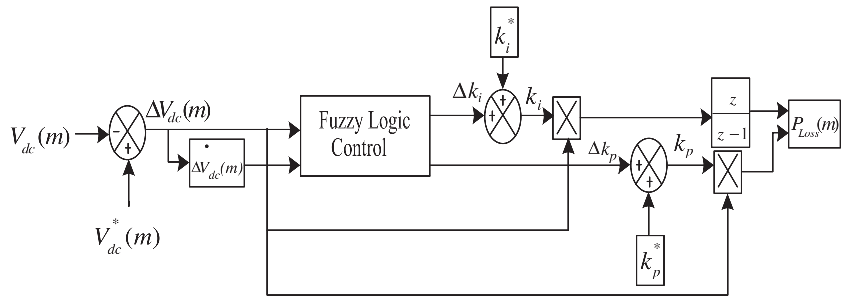

Fig. 5. Schematic of adaptive fuzzy logic PI controller.

For α–β PCC voltage components, self-tuning filtering has been applied. This filter allows attenuation of any harmonic component of the distorted PCC voltages resulting in performance improvement of the compensator.

For a three phase system, an instantaneous power can be defined as,

$$p = v_a(t)i_a(t) + v_b(t)i_b(t) + v_c(t)i_c(t) \tag{18}$$

After computation of the fundamental voltage and current components as $\bar{v}_{\alpha\beta}(t)$ and $\bar{i}_{\alpha\beta}(t)$, fundamental component of instantaneous active power is defined as,

$$\bar{p} = \overline{v_\alpha}(t)\overline{i_\alpha}(t) + \overline{v_\beta}(t)\overline{i_\beta}(t) \tag{19}$$

Similarly, the fundamental component of instantaneous reactive power can be written as,

$$\bar{q} = -\overline{v_\beta}(t)\overline{i_\alpha}(t) + \overline{v_\alpha}(t)\overline{i_\beta}(t) \tag{20}$$

As shown in Fig. 2, reference supply currents $i^*_{s\alpha}$ and $i^*_{s\beta}$ in α–β coordinate can be expressed as,

$$\begin{bmatrix} i^*_{s\alpha} \\ i^*_{s\beta} \end{bmatrix} = \frac{1}{\Delta}\begin{bmatrix} \overline{v_\alpha} & -\overline{v_\beta} \\ \overline{v_\beta} & \overline{v_\alpha} \end{bmatrix}\begin{bmatrix} \bar{p} \\ \bar{q} \end{bmatrix} \tag{21}$$

For power factor correction, fundamental component of instantaneous reactive power ($\bar{q}$) is taken as zero.

These currents can be transformed into a–b–c quantities to find the three phase reference supply currents using reverse Clark's transformation [22] as,

$$\begin{bmatrix} i^*_{sa} \\ i^*_{sb} \\ i^*_{sc} \end{bmatrix} = \sqrt{\frac{2}{3}}\begin{bmatrix} 1 & 0 & 1/\sqrt{2} \\ -1/2 & \sqrt{3}/2 & 1/\sqrt{2} \\ -1/2 & -\sqrt{3}/2 & 1/\sqrt{2} \end{bmatrix}\begin{bmatrix} i^*_{s\alpha} \\ i^*_{s\beta} \\ i^*_0 \end{bmatrix} \tag{22}$$

where i^*_0 is the zero sequence current which is zero in three phase three wire system.

These reference supply currents are compared with the sensed supply currents in the hysteresis based current controller to generate switching pulses for VSC of DSTATCOM.

Design of adaptive fuzzy logic controller for DC bus voltage control

PI (Proportional Integral) controllers are used in industries provide good performance once tuned when the parameters used are not of much variations. However, when one applies these PI controllers for nonlinear systems as conditions vary, further tuning is required. Henceforth, a supervisory control of gains of PI controller through the fuzzy logic is presented to improve the performance of the system during transients [35].

Two inputs to the fuzzy logic controller are chosen as an error in DC bus voltage and the derivative of error in DC bus voltage respectively. The value of $k_p(m-1)$ and $k_i(m-1)$ are initialized from various inferences and then the gains achieved from fuzzy calculation are added to get the modified value as $k_p(m)$ and $k_i(m)$.

$$\begin{aligned} k_p(m) &= k_p(m-1) + \Delta k_p(m-1) \\ k_i(m) &= k_i(m-1) + \Delta k_i(m-1) \end{aligned} \tag{23}$$

where Δk_p and Δk_i are the incremental changes in PI controller gains obtained from the fuzzy logic controller.

A schematic of adaptive fuzzy logic controller is shown in Fig. 4 where the two inputs at mth sampling instant are $\Delta V_{dc}(m)$ and its derivative $\Delta\dot{V}_{dc}(m)$. Its optimized output values are k_p and k_i. According to the schematic shown in Fig. 5 one can write the following expression for adaptive fuzzy logic controller [34] as,

$$\Delta V_{dc}(m) = V^*_{dc}(m) - V_{dc}(m) \tag{24}$$

$$P_{Loss}(m) = P_{Loss}(m-1) + k_p\{\Delta v_{dc}(m) - \Delta v_{dc}(m-1)\} + k_i\Delta v_{dc}(m) \tag{25}$$

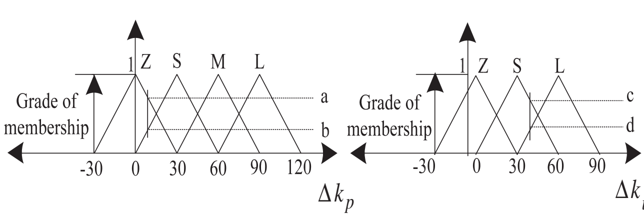

Fig. 6. Membership function for Δk_p and Δk_i .

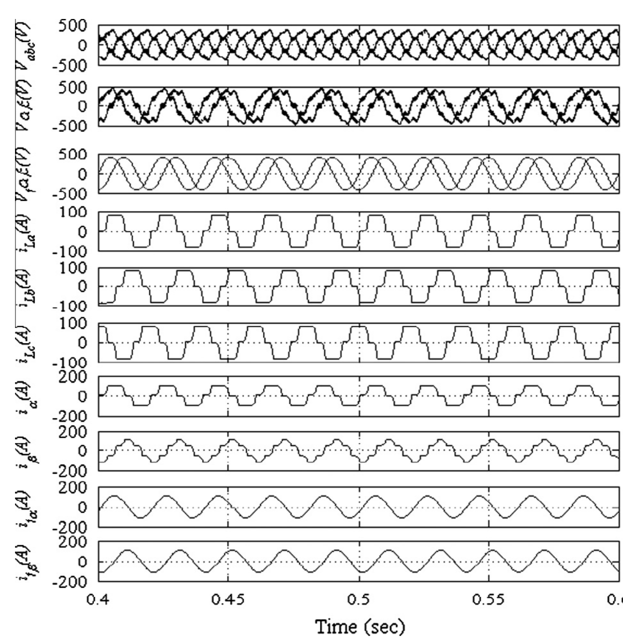

Fig. 7. Fundamental voltages and currents extraction using STF based IRPT control algorithm in DSTATCOM under distorted PCC voltages.

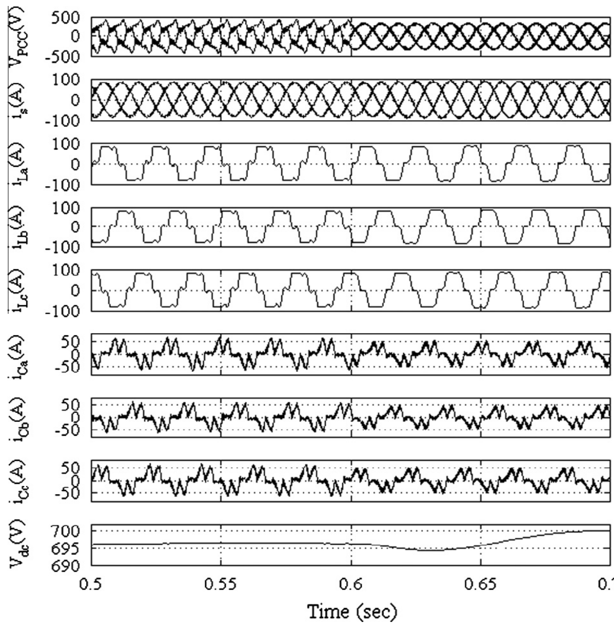

Fig. 8. Performance of DSTATCOM under distorted PCC voltages using conventional PI controller at balanced non-linear load.

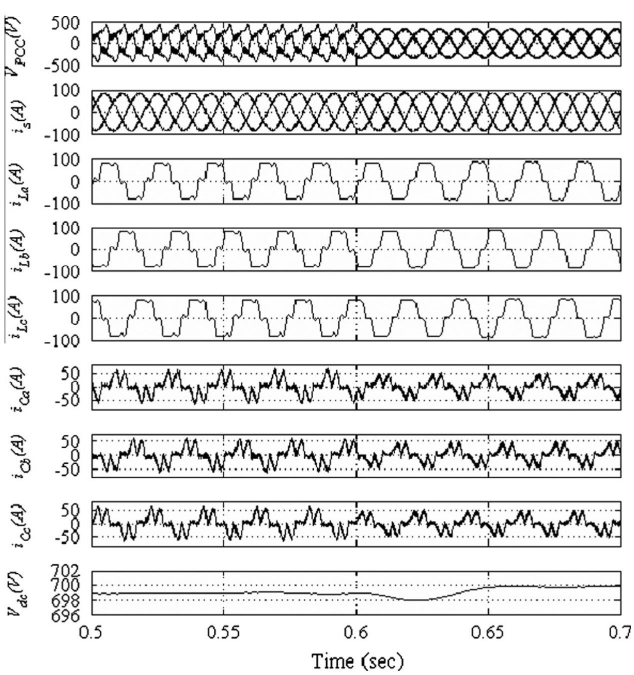

Fig. 9. Performance of DSTATCOM under distorted PCC voltages using adaptive fuzzy logic controller at balanced non-linear load.

where k_p is the proportional gain constant and k_i is the integral gain constant as given in Eq. (23) and $V_{dc}(m)$, $V^*_{dc}(m)$ and $\Delta V_{dc}(m)$ are sensed, reference and error signal of DC link voltage at mth sampling instant respectively.

The output of the adaptive fuzzy logic controller accounts for the losses in DSTATCOM, and it is considered as the loss component of these supply currents. This component $P_{Loss}(m)$ given in Eq. (25) is added with the average real power $(\bar{p})$ in Eq. (21) for controlling the DSTATCOM.

In the proposed fuzzy logic controller, the input variables $\Delta V_{dc}(m)$ and its derivative $\Delta \dot{V}_{dc}(m)$ are set as (negative large, negative medium, negative small, zero, positive large, positive

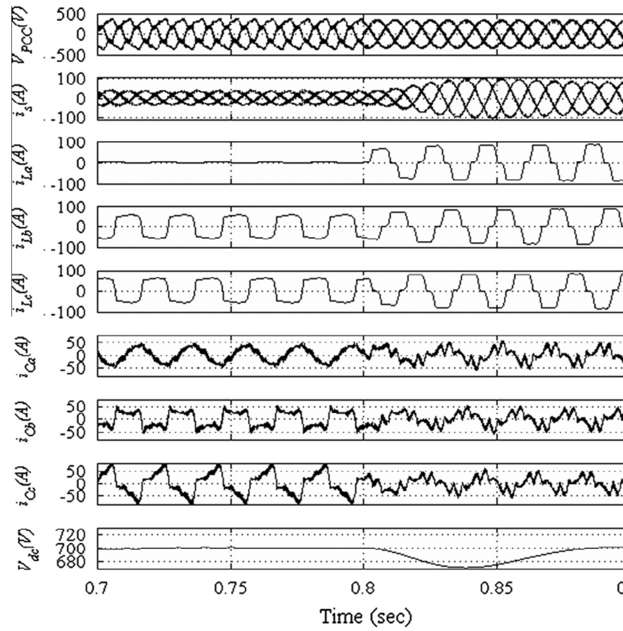

Fig. 10. Performance of DSTATCOM under distorted PCC voltages using conventional PI controller at unbalanced non-linear load.

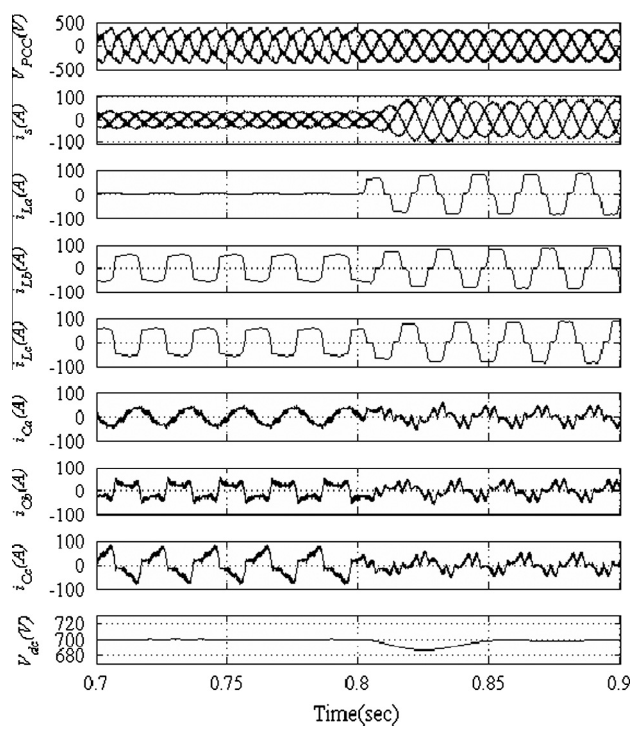

Fig. 11. Performance of DSTATCOM under distorted PCC voltages using adaptive fuzzy logic controller at unbalanced non-linear load.

medium, positive small) and respective abbreviations are (NL, NM, NS, Z, PL, PM, PS}. According to the rules IF-THEN form is used to obtain Δk_p and Δk_i values. Here PS for $\Delta V_{dc}(m)$ is defined as the condition when the DC bus voltage is deviating from the reference value with a small amount which is greater than the sensed value and NS is defined as the condition when the DC bus voltage of VSC of DSTATCOM is deviating from the reference value which is smaller than the sensed value and similarly other abbreviations can be defined.

The rule structure is formed by taking the following important points into consideration.

(1) If the error is small and the derivative of error is positive small and DC bus voltage is deviating from the sensed value then increase k_p with a small amount.
(2) If the error is small and the derivative of error is positive small and DC bus voltage is approaching the sensed value then increase k_i with a small amount to reduce steady state error.
(3) When the error and the derivative of error are positive medium or negative medium, in order to reduce the overshoot of system response, k_p and k_i should not be too big. The value of k_p should be medium and k_i should be small to ensure good system response.

In the membership functions of $\Delta V_{dc}(m)$ and $\Delta \dot{V}_{dc}(m)$, the value of $\Delta V(m)$ and its derivative $\Delta \dot{V}_{dc}(m)$ is in the range (−700, 700). In the membership functions shown in Fig. 6, the values of Δk_p and Δk_i are considered in the range (−30, 120) and (−30, 90). A grade of membership (a value between zero and one), which measures the compatibility of the signal to the membership function, is assigned to the signal. In the triangular functions shown in Fig. 5, the values of points a and b represent the grade of membership of the Δk_p in the Z and S functions, and the values of points *c* and *d* represent the grade of membership of the Δk_i in S and L functions. The sum of *a* and *b*, and the sum of *c* and *d*, are to be equal to one for triangular membership functions.

IF $\Delta V_{dc}(m)$ is NL and $\Delta \dot{V}_{dc}(m)$ is NL then Δk_p is L and Δk_i is S
IF $\Delta V_{dc}(m)$ is NL and $\Delta \dot{V}_{dc}(m)$ is NM then Δk_p is L and Δk_i is S
IF $\Delta V_{dc}(m)$ is NL and $\Delta \dot{V}_{dc}(m)$ is NS then Δk_p is L and Δk_i is S
IF $\Delta V_{dc}(m)$ is NL and $\Delta \dot{V}_{dc}(m)$ is Z then Δk_p is M and Δk_i is S
IF $\Delta V_{dc}(m)$ is NL and $\Delta \dot{V}_{dc}(m)$ is PS then Δk_p is S and Δk_i is Z
IF $\Delta V_{dc}(m)$ is NL and $\Delta \dot{V}_{dc}(m)$ is NM then Δk_p is S and Δk_i is Z
IF $\Delta V_{dc}(m)$ is NL and $\Delta \dot{V}_{dc}(m)$ is PL then Δk_p is Z and Δk_i is Z

Similarly when $\Delta V_{dc}(m)$ is NM, NS, Z, PL, PM, PS individually one can have 49 rules for different Δk_p and Δk_i values.

Simulation and experimental results

Simulation model of a DSTATCOM is developed for a three-phase distribution system in MATLAB environment using SIMULINK and Sim Power System (SPS) toolboxes. The performance of STF based IRPT with adaptive fuzzy logic control algorithm is simulated under distorted PCC voltages at both balanced and unbalanced nonlinear loads.

A real time implementation of DSTATCOM using a three-leg VSC is developed to validate the proposed control algorithm. It is connected in parallel to the three phase AC mains. Hall Effect current sensors (EL50P1 BB) and voltage sensors (EM010 BB) are used for sensing load currents, supply currents, PCC voltages and DC bus voltage of VSC of DSTATCOM. A STF based IRPT control algorithm with adaptive fuzzy logic is used for the control of DSTATCOM using a DSP (Digital signal Processor dSPACE 1104). A power analyzer (Fluke 43B) and digital oscilloscope (an Agilent made-DSO-6014A) are used as recording instruments. Simulation and Hardware implementation parameters are defined in Appendices A and B respectively.

Performance of STF based control algorithm of DSTATCOM under distorted PCC voltages

Fundamental voltages and currents extraction during distorted PCC voltages conditions are shown in Fig. 7. In this case, 5th and 7th harmonic components of 0.2 p.u. magnitude are injected into the PCC voltages. Hence the input voltages (v_α, v_β) and current signals (i_α, i_β) to the STF are composed of fundamental with harmonics components and after filtering the output voltages ($v_{f\alpha}, v_{f\beta}$) and current signals ($i_{f\alpha}, i_{f\beta}$) contain only fundamental components which can be clearly observed from Fig. 7, which verifies the effectiveness of STF based IRPT control algorithm used in DSTATCOM.

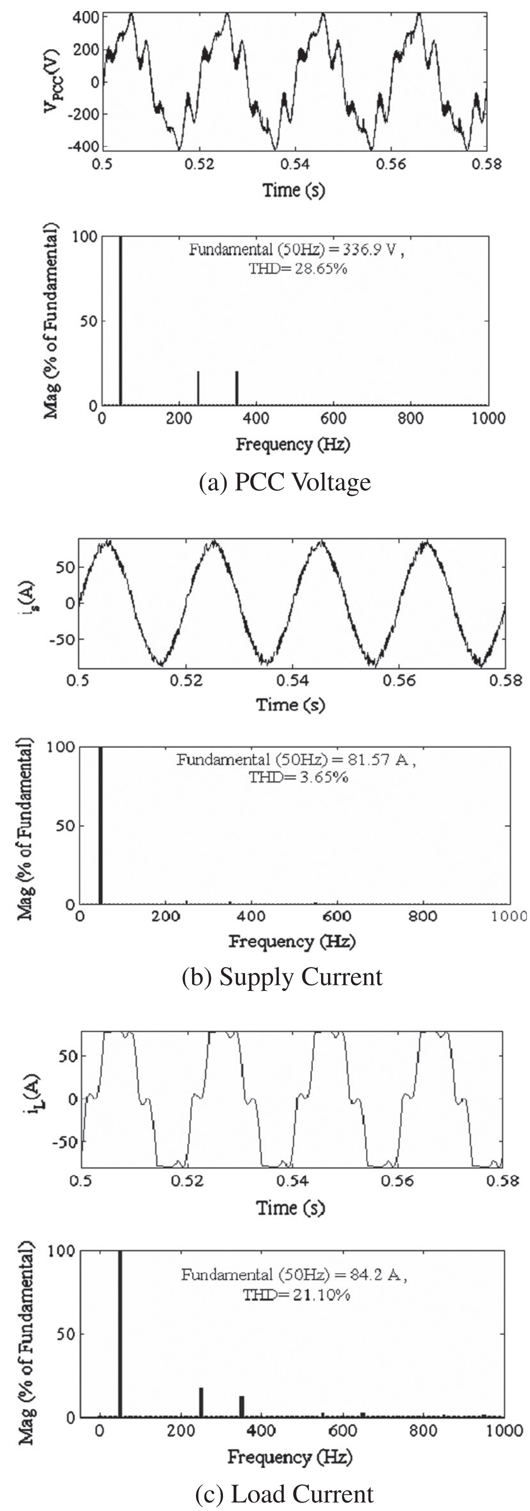

Fig. 12. Waveforms and harmonics spectra of (a) PCC voltage. (b) Supply current. (c) Load current under distorted PCC voltages under non-linear load using adaptive fuzzy logic controller.

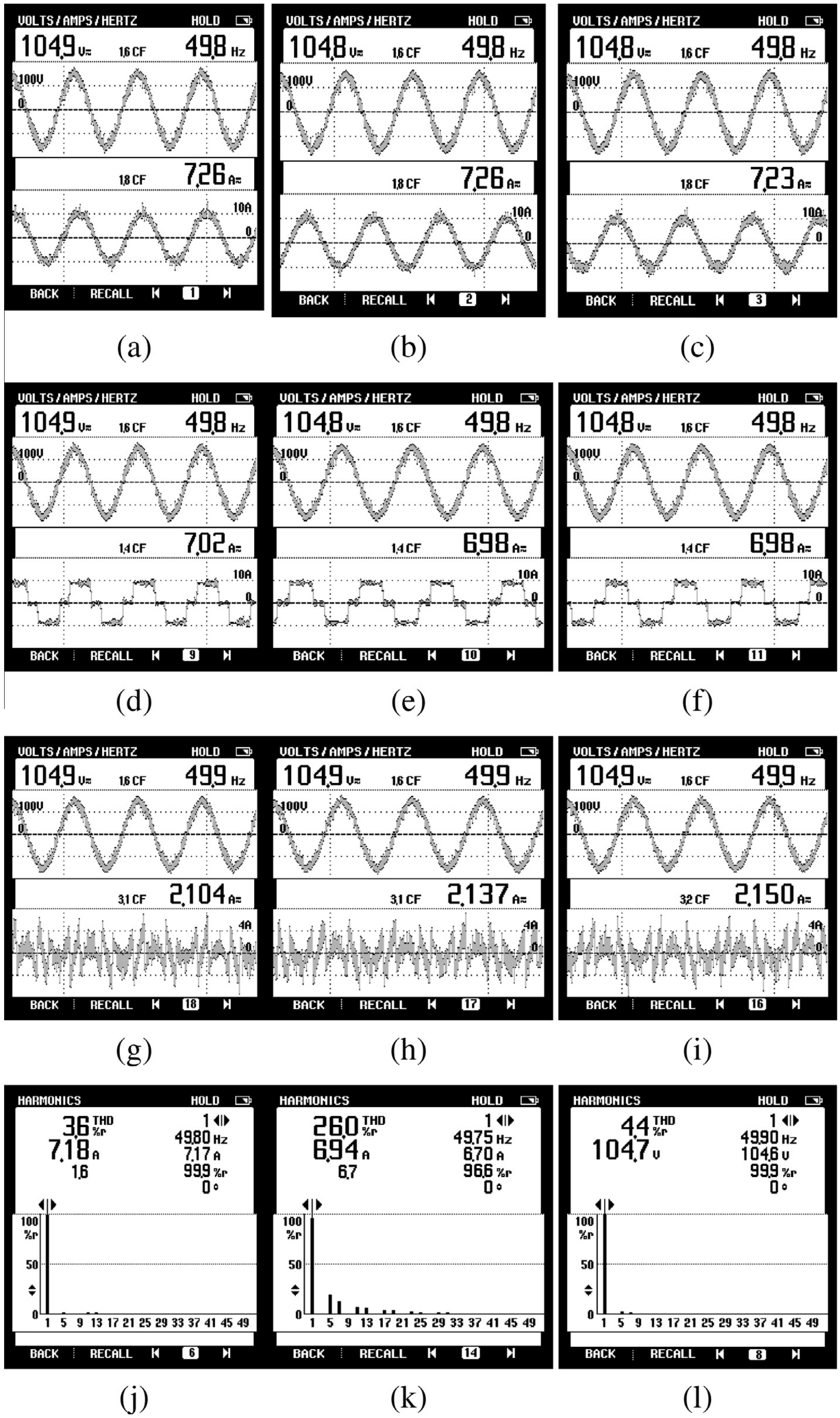

Fig. 13. Experimental performance of DSTATCOM under nonlinear load (a–c) i_{sa}, i_{sb} and i_{sc} with v_{ab} (d–f) i_{La}, i_{Lb} and i_{Lc} (g–i) i_{Ca}, i_{Cb} and i_{Cc} (j–l) Harmonic spectra of i_{sa}, i_{La} and v_{ab}.

Fig. 13(a–i) shows the waveforms of phase 'a' PCC voltages (v_{abc}) with supply currents (i_{sa}, i_{sb}, i_{sc}), load currents (i_{La}, i_{Lb}, i_{Lc}) and compensating currents (i_{Ca}, i_{Cb}, i_{Cc}) under nonlinear loads. In Fig. 13(j–l), THD (Total Harmonic Distortions) of 'a' phase supply current, load current and PCC voltage are observed as 3.6%, 26.0% and 4.4% respectively. These results demonstrate satisfactory performance of the STF based IRPT control algorithm where THD of supply current is 3.6% even if the THD of PCC voltage is 4.4%.

Performance of adaptive fuzzy logic controller

Figs. 8 and 9 show the waveforms of three phase PCC voltages (v_{pcc}) with supply currents (i_s), load currents (i_{La}, i_{Lb}, i_{Lc}), compensating currents (i_{Ca}, i_{Cb}, i_{Cc}) and DC link voltage (V_{dc}) under nonlinear loads using conventional PI controller and adaptive fuzzy logic controller. In both the cases from 0.5 s to 0.6 s, 5th and 7th harmonic components of 0.2 p.u. magnitude are injected in the PCC

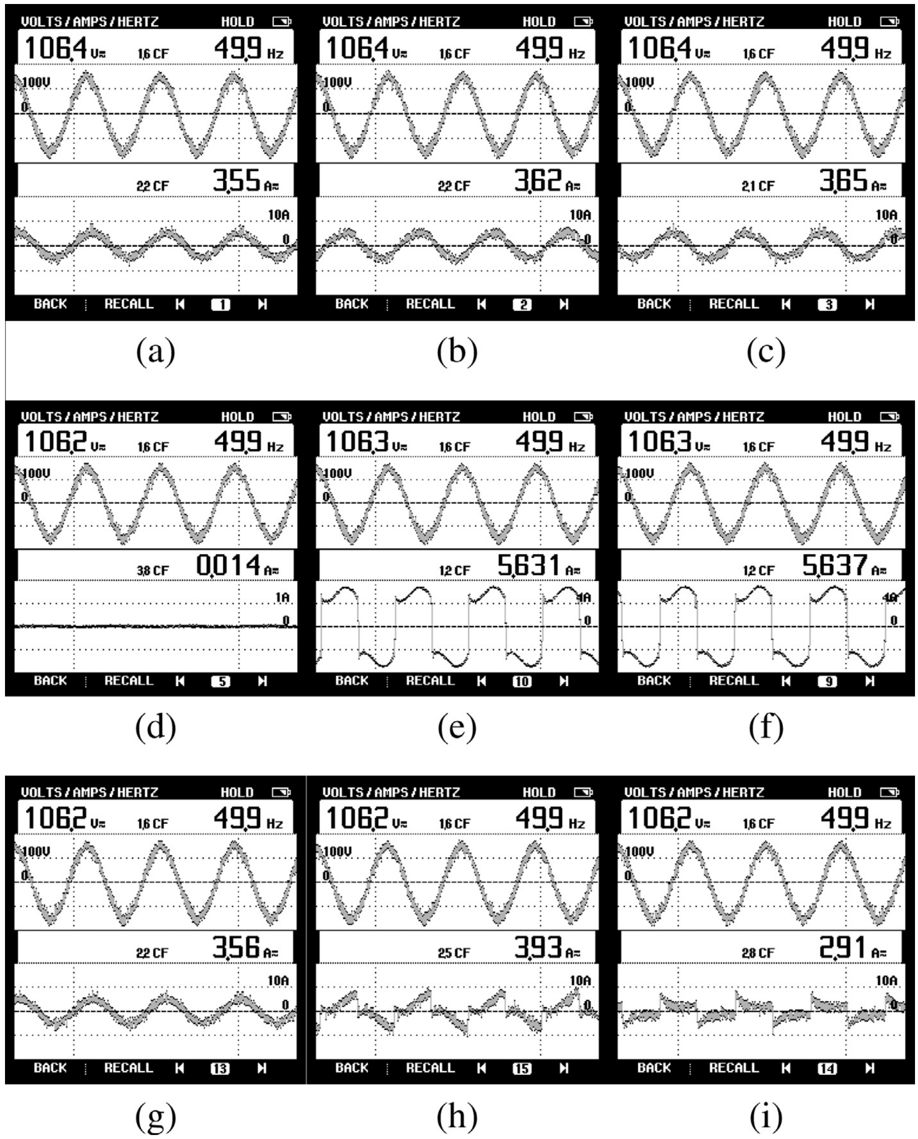

Fig. 14. Experimental performance of DSTATCOM under unbalanced nonlinear load (a–c) i_{sa}, i_{sb} and i_{sc} with v_{ab} (d–f) i_{La}, i_{Lb} and i_{Lc} (g–i) i_{Ca}, i_{Cb} and i_{Cc}.

Table 1
Performance of DSTATCOM.

Performance parameters	Distorted PCC voltages at balanced non-linear load	Distorted PCC voltages at unbalanced non-linear load
PCC voltage (V), % THD	336.9 V, 28.65%	337.9 V, 14.59%
Supply current (A), % THD	81.57 A, 3.65%	35.59 A, 4.42%
Load current (A), % THD	84.20 A, 21.10%	69.21 A, 31. 91%

voltages. One can observe from Figs. 8 and 9 that in case of conventional PI controller DC link bus voltage has an undershoot of 7 V whereas in case of adaptive fuzzy logic controller an undershoot is only of 2 V for the DC link bus voltage which verifies the effectiveness of adaptive fuzzy logic controller in case of distorted PCC voltages. Again Figs. 10 and 11 show the waveforms of three phase PCC voltages (v_{pcc}) with supply currents (i_s), load currents (i_{La}, i_{Lb}, i_{Lc}), compensating currents (i_{Ca}, i_{Cb}, i_{Cc}) and DC link voltage (V_{dc}) under unbalanced nonlinear loads using conventional PI controller and adaptive fuzzy logic controller. In both the cases from 0.7 s to 0.8 s, 5th and 7th harmonic components of 0.1 p.u. magnitude are injected into the PCC voltages at the same time the load is unbalanced from 0.7 s to 0.8 s which is a worst condition in a distribution system. From Figs. 10 and 11, one can infer that in case of PI controller, DC link bus voltage has an undershoot of 30 V whereas in case of adaptive fuzzy logic controller an undershoot is only of 15 V for DC link bus voltage and also in case of conventional PI controller, the DC bus voltage has taken 4 cycles to get settled down whereas in case of adaptive fuzzy logic controller DC bus has taken only 2 cycles to get settled down which verifies the effectiveness of adaptive fuzzy logic controller in case of distorted PCC voltages under unbalanced load conditions.

The waveforms of supply currents (i_{sa}, i_{sb}, i_{sc}), load currents (i_{La}, i_{Lb}, i_{Lc}) and compensating currents (i_{Ca}, i_{Cb}, i_{Cc}) with PCC line voltage (v_{ab}) are shown in Fig. 14(a)–(i) under unbalanced nonlinear loads. Unbalanced loads can be observed after load removal of

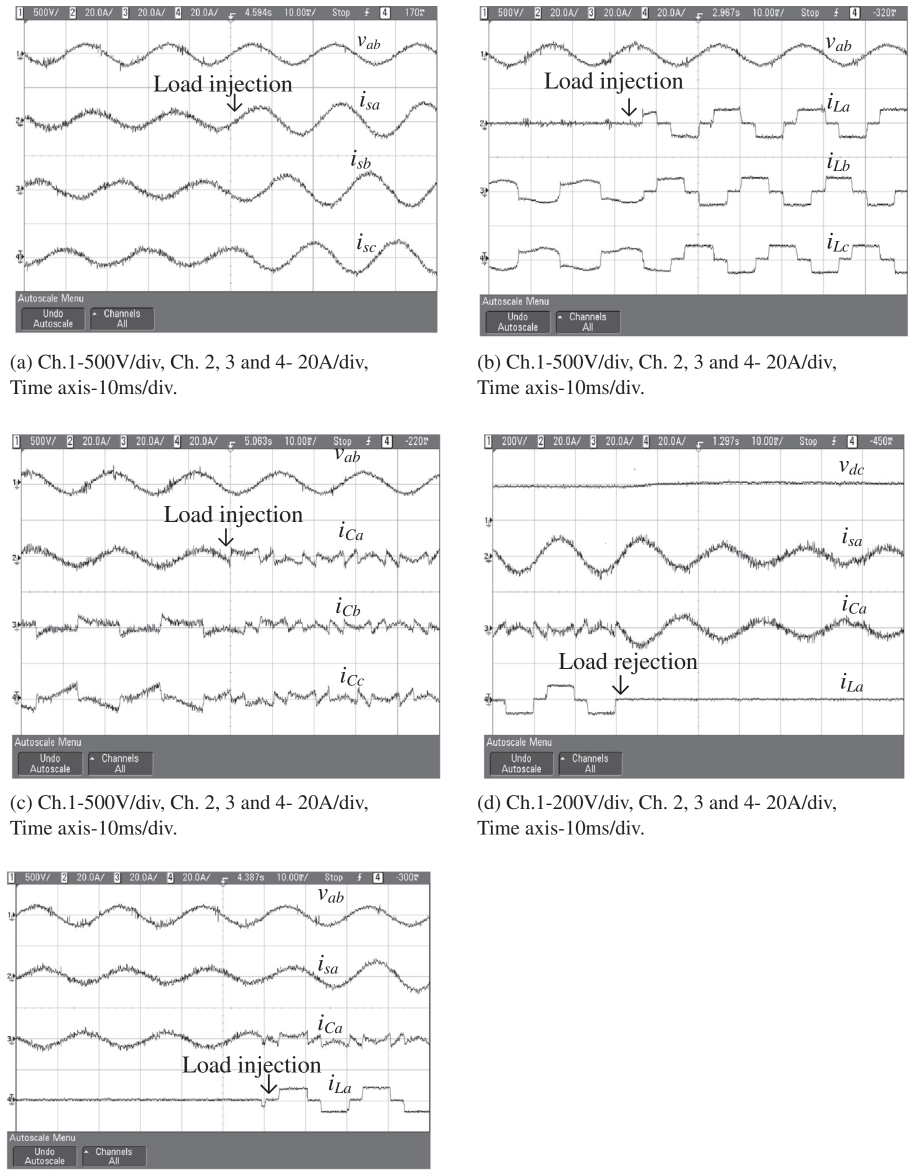

(a) Ch.1-500V/div, Ch. 2, 3 and 4- 20A/div, Time axis-10ms/div.

(b) Ch.1-500V/div, Ch. 2, 3 and 4- 20A/div, Time axis-10ms/div.

(c) Ch.1-500V/div, Ch. 2, 3 and 4- 20A/div, Time axis-10ms/div.

(d) Ch.1-200V/div, Ch. 2, 3 and 4- 20A/div, Time axis-10ms/div.

(e) Ch.1-500V/div, Ch. 2, 3 and 4- 20A/div, Time axis-10ms/div.

Fig. 15. Dynamic performance of DSTATCOM in phase 'a' (a) v_{ab}, i_{sa}, i_{sb} and i_{sc} (b) v_{ab} i_{La}, i_{Lb} and i_{Lc} (c) v_{ab} i_{Ca}, i_{Cb} and i_{Cc} (d) v_{dc} i_{sa}, i_{Ca} and i_{La} (e) v_{ab} i_{sa}, i_{La} and i_{Ca}.

phase 'a' load. These steady state results show balanced supply currents under unbalanced loads demonstrating satisfactory load balancing even under non-linear load.

Dynamic performance of DSTATCOM

After observing Fig. 12(a–c), it can be inferred that the THD (Total Harmonic distortion) of supply current is 3.65% where as THD of PCC voltage is 28.65% and THD of load current is 21.10%. Performance of DSTATCOM for different PCC voltages and load conditions are shown in Table 1. The supply current is in phase with PCC voltage which is clearly shown in Fig. 11 to achieve unity power factor. These results show balanced sinusoidal supply currents under distorted PCC voltages and unbalanced nonlinear load conditions. Simulation results therefore have verified the effectiveness of the proposed control algorithm under distorted PCC voltages at nonlinear unbalanced load conditions.

The waveforms of supply currents (i_{sa},i_{sb},i_{sc}), load currents (i_{La},i_{Lb},i_{Lc}) and compensating currents (i_{Ca},i_{Cb},i_{Cc}) with PCC line voltage (v_{ab}) are shown in Fig. 15(a–c) under varying loads. The DC bus voltage (v_{dc}) with supply current (i_{sa}), compensating current (i_{Ca}) and load current (i_{La}) are shown in Fig. 15(d) during load rejection. The PCC voltage (v_{ab}) with supply current (i_{sa}), compensating current (i_{Ca}) and load current (i_{La}) are shown in Fig. 15(e) during load injection. It shows balanced supply currents when load currents are not balanced and it proves the fast action of control algorithm at the load application. From these results one can observe the fast and effective control of adaptive fuzzy logic controller used for DC bus voltage control of VSC of DSTATCOM. These results have also shown the satisfactory performance of control algorithm used in DSTATCOM under unbalanced nonlinear loads and distorted PCC voltages.

Conclusion

A self tuning filter based IRPT control algorithm with an adaptive fuzzy logic controller has been used in VSC based DSTATCOM for power quality improvement in a distribution system. The use of self tuning filter has a satisfactory performance of a DSTATCOM which has been validated by both simulation and experimental results. Since it perfectly extracts the fundamental component of current under distorted voltages condition, it has been found as an effective solution to power quality problems. For DC bus control of VSC of DSTATCOM, an adaptive fuzzy logic controller has been used which has regulated the DC voltage to the desired level without much overshoot and undershoot under both distorted and unbalanced load currents conditions. The adaptive fuzzy logic controller has also demonstrated its effectiveness in regulating DC voltage under supply voltage fluctuation. The simulation and experimental results have demonstrated the major advantages of proposed control algorithm.

Appendix A

AC mains: 3-Phase, 415 V (L–L), 50 Hz, Non-linear loads: Three phase full bridge diode based rectifier with $R = 6\,\Omega$ and $L = 100$ mH; Self tuned filter constant factor (η) = 20; dc bus capacitance: 2000 μF; Reference dc bus voltage: 700 V; Interfacing inductor (L_f) = 2 mH; Ripple filter: $R_f = 5\,\Omega$, $C_f = 10$ μF; Gains of dc bus PI controller: $k_p = 40$, $k_i = 10$; Cut off frequency of low pass filter used in dc bus = 20 Hz.

Appendix B

Non-ideal AC mains: 3-Phase, 110 V (L–L), 50 Hz, Non-linear loads: Three phase full bridge diode based rectifier with $R = 40\,\Omega$ and $L = 100$ mH; Self tuned filter constant factor (η) = 20; dc bus capacitance: 1650 μF; Reference dc bus voltage: 200 V; interfacing inductor (L_f) = 2.5 mH; Ripple filter: $R_f = 5\,\Omega$, $C_f = 10$ μF; Cut off frequency of low pass filter used in dc bus = 20 Hz; Sampling time of DSP (t_s) = 50 μs.

Appendix C

Detailed expressions of Eqs. (11) and (12) i.e. $\bar{v}_\alpha(t)$ *and* $\bar{v}_\beta(t)$

By substituting Eqs. (3) and (4) into Eqs. (11) and (12) the following expressions from STF output can be obtained [23],

$$\bar{v}_\alpha(t) = \sqrt{\frac{3}{2}}V_1(1 - e^{-\eta t})\sin(wt + \phi_1) + \sqrt{\frac{3}{2}}\sum_{n=2}^{\infty}\left[\frac{V_n}{\sqrt{1 + \{\frac{(1-n)w}{\eta}\}^2}}\right] \times [\sin(nwt + \phi_n + \delta_n) - e^{-\eta t}\sin(wt + \phi_n + \delta_n)] \quad (26)$$

$$\bar{v}_\beta(t) = -\sqrt{\frac{3}{2}}V_1(1 - e^{-\eta t})\cos(wt + \phi_1) - \sqrt{\frac{3}{2}}\sum_{n=2}^{\infty}\left[\frac{V_n}{\sqrt{1 + \left\{\frac{(1-n)w}{\eta}\right\}^2}}\right] \times [\cos(nwt + \phi_n + \delta_n) - e^{-\eta t}\cos(wt + \phi_n + \delta_n)] \quad (27)$$

where $\delta_n = \tan^{-}\left\{\frac{(1-n)w}{\eta}\right\}$.

From Eqs. (26) and (27) one can examine the influence of parameter η on the STF dynamic performances. One can notice that time constant (τ) of STF is equal to $1/\eta$, which means transient time is decreased with the increment in 'η'. Again, it is observed that there is no phase delay (δ_n) in the estimation of fundamental component ($n = 1$) of PCC voltages.

From Eqs. (26) and (27), it is seen that the STF reduces the amplitude of the harmonics component with the factor equal to $1/\sqrt{1 + \left\{\frac{(1-n)w}{\eta}\right\}^2}$ for 2nd and higher order harmonics. This factor is equal to 1 for fundamental component which signifies the effectiveness of STF.

References

[1] Fuchs Ewald F, Mausoum Mohammad AS. Power quality in power systems and electrical machines. London: Elsevier Academic Press; 2008.
[2] Padiyar KR. FACTS controllers in power transmission and distribution. New Delhi: New Age International; 2008.
[3] Brenna M, Foiadelli F, Zaninelli D. Electromagnetic model of high speed railway lines for power quality studies. IEEE Trans Power Syst Aug. 2010;25(3):1301–8.
[4] Chen Cheng I, Chen Yeong C. Comparative study of harmonic and inter harmonic estimation methods for stationary and time-varying signals. IEEE Trans Industr Electron Jan. 2014;61(1):397–404.
[5] Sannino Ambra, Svensson Jan, Larsson Tomas. Review power electronic solutions to power quality problems. J Electr Power Syst Res 2003;66:71–82.
[6] Singh Bhim, Al-Haddad K, Chandra A. A review of active filters for power quality improvement. IEEE Trans Industr Electron 1999;46(5):960–71.
[7] IEEE recommended practices and requirement for harmonic control on electric power system, IEEE Std. 519; 1992.
[8] Singh B, Adya A, Mittal AP, Gupta JRP. Analysis, simulation and control of DSTATCOM in three-phase, four-wire isolated distribution systems. In: Proc of IEEE Power India Conference; 2006. p. 1–6.
[9] Tang Yi, Loh Poh Chiang, Wang Peng, Choo Fook Hoong, Gao Feng, Blaabjerg F. Generalized design of high performance shunt active power filter with output LCL filter. IEEE Trans Industr Electron March 2012;59(3):1443–52.
[10] Bhattacharya A, Chakraborty C, Bhattacharya S. Parallel-connected shunt hybrid active power filters operating at different switching frequencies for improved performance. IEEE Trans Industr Electron 2012;59(11):4007–19.
[11] Rahmani S, Hamadi A, Al-Haddad K. A lyapunov-function-based control for a three-phase shunt hybrid active filter. IEEE Trans Industr Electron 2012;59(3):1418–29.
[12] Montero MIM, Cadaval ER, Gonzalez FB. Comparison of control strategies for shunt active power filters in three-phase four-wire systems. IEEE Trans Power Electron 2007;22(1):229–36.
[13] Kanjiya P, Khadkikar V, Zeineldin HH. A non-iterative optimized algorithm for shunt active power filter under distorted and unbalanced supply voltages. IEEE Trans Industr Electron Dec. 2013;60(12):5376–90.
[14] Trinh Q-N, Lee H-H. An advanced current control strategy for three-phase shunt active power filters. IEEE Trans Industr Electron Dec. 2013;60(12):5400–10.
[15] Singh R, Singh DK. Simulation of DSTATCOM for voltage fluctuation. In: Proc of second international conference on advanced computing and communication technologies; 2012. p. 225–30.
[16] Hu Haibing, Wei Shi, Lu Ying, Xing Yan. Design considerations for DSP-controlled 400 Hz shunt active power filter in an aircraft power system. IEEE Trans Industr Electron 2012;59(9):3624–34.
[17] Rajagopal V, Singh B, Kasal GK. Electronic load controller with power quality improvement of isolated induction generator for small hydro power generation. IET Renew Power Gener 2011;5(2):202–13.
[18] Longhui Wu, Fang Zhuo, Pengbo Zhang, Hongyu Li, Zhaoan Wang. Study on the influence of supply-voltage fluctuation on shunt active power filter. IEEE Trans Power Delivery 2007;22(3):1743–9.
[19] de Araujo Ribeiro RL, de Azevedo CC, de Azevedo CC, de Sousa RM. A robust adaptive control strategy of active power filters for power-factor correction, harmonic compensation, and balancing of nonlinear loads. IEEE Trans Power Electron Feb. 2012;27(2):718–30.
[20] Depenbrock M, Staudt V, Wrede H. A theoretical investigation of original and modified instantaneous power theory applied to four-wire systems. IEEE Trans Indus Appl 2003;39(4):1160–8.
[21] Herrera RS, Salmeron P. Instantaneous reactive power theory: a reference in the nonlinear loads compensation. IEEE Trans Industr Electron June 2009;56(6):2015–22.
[22] Pigazo Alberto, Moreno Victor M, Estebanez Emilio J. A recursive park transformation to improve the performance of synchronous reference frame controllers in shunt active power filters. IEEE Trans Power Electron September 2009;24(9):2065–75.
[23] Abdusalam Mohamed, Poure Philippe, Karimi Shahram, Saadate Shahrokh. New digital current generation for shunt active power filter under distorted voltage conditions. J Electr Power Syst Res May 2009;79(5):759–65.
[24] Singh BN, Chandra A, Haddad K. Performance comparison of two current control techniques applied to an active power filter. In: International conference on harmonics and quality of power. Athens; 1998. p. 133–8.
[25] Mishra MK, Ghosh A, Joshi A. Operation of a DSTATCOM in voltage control mode. IEEE Trans Power Delivery Jan 2003;18(1):258–64.
[26] Freijedo FD, Doval-Gandoy J, Lopez O, Fernandez-Comesana P, Martinez Penalver C. A signal-processing adaptive algorithm for selective current harmonic cancellation in active power filters. IEEE Trans Industr Electron 2009;56(8):2829–40.
[27] Singh B, Kumar S. Control of DSTATCOM using IcosΦ algorithm. In Proc of 35th annual conference of IEEE industrial electronics (IECON); 2009. p. 322–7.
[28] Singh Bhim, Singhal Varun. Fuzzy pre-compensated PI control of active filters. J Power Electron 2008;8(2):141–7.
[29] Suryanarayana H, Mishra MK. Fuzzy logic based supervision of DC link PI control in a DSTATCOM. In: Proc of annual IEEE India conference (INDICON), vol. 2; 2008. p. 453–8.

[30] Longhui Wu, Fang Zhuo, Pengbo Zhang, Hongyu Li, Zhaoan Wang. Study on the influence of supply-voltage fluctuation on shunt active power filters. IEEE Trans Power Delivery 2007;22(3).

[31] Hong-Seok, Hyun-Gyu P, Kwanghee N. An instantaneous phase angle detection algorithm under unbalanced line voltage condition. In: Proc of IEEE 30th annual power electronics specialist conference, vol. 1; 1999. p. 533–7.

[32] Singh BN, Chandra A, Al-Haddad K. DSP-based indirect current-controlled STATCOM. Part I: Evaluation of current control techniques. IEE Proc Electr Power Appl 2000;147:107–12.

[33] Ajami A, Hosseini HS. Application of a Fuzzy controller for transient stability enhancement of ac transmission system by STATCOM. In: Proc of international joint conference SICE-ICASE; 2006. p. 6059–63.

[34] Tzafestas S, Papanikolopoulos NP. Incremental fuzzy expert PID control. IEEE Trans Industr Electron 1990;37(5):365–71.

[35] Passino KM, Yurkovich S. Fuzzy control. Menlo-Park, California: Addison-Wesley Longman Inc.; 1998.

[36] Montero M, Cadaval ER, Gonzalez F. Comparison of control strategies for shunt active power filters in three-phase four-wire systems. IEEE Trans Power Electron 2007;22:229–36.

[37] George S, Agarwal V. A DSP based optimal algorithm for shunt active filter under non sinusoidal supply and unbalanced load conditions. IEEE Trans Power Electron 2007;22:593–601.

[38] Chang GW, Yeh CM. Optimisation-based strategy for shunt active power filter control under non-ideal supply voltages. IEE Proc Electr Power Appl 2005;152:182–90.

[39] Divan DM, Bhattacharya S, Banerjee B. Synchronous frame harmonic isolator using active series filter. In: Proc eur power electron. conf; 1991. p. 3030–5.

[40] Newman M, Zmood M, Holmes D. Stationary frame harmonic reference generation for active filter systems. In: Proceedings of IEEE 17th applied power electronics conference APEC'02, vol. 2; 2002. p. 1054–60.

[41] Pigazo A, Moreno VM, Estebanez EJ. A recursive park transformation to improve the performance of synchronous reference frame controllers in shunt active power filters. IEEE Trans Power Electron 2009;24(9):2065–75.

[42] Bojoi RI, Griva G, Bostan V, Guerriero M, Farina F, Profumo F. Current control strategy for power conditioners using sinusoidal signal integrators in synchronous reference frame. IEEE Trans Power Electron 2005;20(6):1402–12.